

Solution Structure of the E200K Variant of Human Prion Protein

IMPLICATIONS FOR THE MECHANISM OF PATHOGENESIS IN FAMILIAL PRION DISEASES*

Received for publication, July 21, 2000, and in revised form, August 15, 2000
Published, JBC Papers in Press, August 22, 2000, DOI 10.1074/jbc.C000483200

Yongbo Zhang[‡], Wieslaw Swietnicki[§], Michael G. Zagorski[‡], Witold K. Surewicz^{§¶}, and Frank D. Sönnichsen[¶]

From the [‡]Department of Chemistry, [§]Institute of Pathology, and [¶]Department of Physiology and Biophysics, Case Western Reserve University, Cleveland, Ohio 44106

Prion propagation in transmissible spongiform encephalopathies involves the conversion of cellular prion protein, PrP^C, into a pathogenic conformer, PrP^{Sc}. Hereditary forms of the disease are linked to specific mutations in the gene coding for the prion protein. To gain insight into the molecular basis of these disorders, the solution structure of the familial Creutzfeldt-Jakob disease-related E200K variant of human prion protein was determined by multi-dimensional nuclear magnetic resonance spectroscopy. Remarkably, apart from minor differences in flexible regions, the backbone tertiary structure of the E200K variant is nearly identical to that reported for the wild-type human prion protein. The only major consequence of the mutation is the perturbation of surface electrostatic potential. The present structural data strongly suggest that protein surface defects leading to abnormalities in the interaction of prion protein with auxiliary proteins/chaperones or cellular membranes should be considered key determinants of a spontaneous PrP^C → PrP^{Sc} conversion in the E200K form of hereditary prion disease.

Spongiform encephalopathies, or prion diseases, are a novel class of neurodegenerative disorders that affect animals and humans. They include scrapie in sheep, bovine spongiform encephalopathy in cattle, and Creutzfeldt-Jakob disease (CJD),¹ Gerstmann-Sträussler-Scheinker disease (GSS), fatal familial insomnia (FFI), and kuru in humans. These diseases may arise sporadically, may be inherited, or may be acquired by transmission of an infectious agent (1, 2).

According to the “protein only” hypothesis (1–3), the key event in the pathogenesis of prion disorders is the conversion of a normal prion protein, PrP^C, into a pathogenic (scrapie) form,

PrP^{Sc}. The latter protein accumulates in the diseased brain and is believed to be the sole component of the infectious prion pathogen. The transition between PrP^C and PrP^{Sc} occurs post-translationally without any detectable covalent modifications to the protein molecule (4). The two protein isoforms have profoundly different physicochemical properties. PrP^C is highly soluble and easily degraded by proteinase K, whereas PrP^{Sc} exists as an insoluble aggregate that is resistant to proteinase K digestion and often has the characteristics of an amyloid (5, 6). These differences in physical properties most likely reflect different conformations of the two isoforms. Indeed, spectroscopic data show that PrP^C is highly α -helical, whereas PrP^{Sc} contains a large proportion of β -sheet structure (7–10).

In addition to biochemical evidence, the protein only hypothesis is supported by experiments showing the resistance of PrP knockout mice to the infectious scrapie agent (11). Another argument in favor of this hypothesis is the link between hereditary human spongiform encephalopathies (*i.e.* familial CJD, GSS, and FFI) and specific mutations in the gene coding for the human prion protein (1, 12). A key to understanding the mechanism by which familial mutations facilitate the pathogenic process is to determine how these mutations affect the conformational structure of prion protein. In the present study, we report the three-dimensional structure of the folded domain of the recombinant human prion protein containing a mutation (E200K) corresponding to the most common familial form of Creutzfeldt-Jakob disease.

EXPERIMENTAL PROCEDURES

Plasmid Construction and Protein Expression and Purification—The E200K mutant was constructed using the QuikChange™ kit (Stratagene, La Jolla, CA) and primers 5'-GAAGTTCACCAAGACCGACGTTAAG-3' and 5'-CTTAACGTCGGTCTTGGTGAAGTTC-3'. The template DNA was the pRSETB vector with the cDNA corresponding to the wild-type huPrP-(90–231) inserted into the multiple cloning site as described previously (13). The protein was expressed, refolded, and purified using the procedures described previously (13). To obtain ¹⁵N/¹³C-labeled protein, bacteria were grown in a minimum medium containing ¹⁵NH₄Cl (1 g/l) and ¹³C₆-glucose (2 g/l) as a sole source of nitrogen and carbon, respectively.

NMR Spectroscopy—Samples for NMR spectroscopy were prepared at a protein concentration of 0.7–0.9 mM in 10 mM d₄-sodium acetate buffer containing 0.005% sodium azide and 10% (v/v) D₂O, pH 4.6. Most NMR measurements were performed at 26 °C on a Varian INOVA 600 spectrometer equipped with a triple-resonance gradient probe. Some ¹⁵N-HSQC, HCCH-total correlation spectroscopy, 100-ms ¹³C-NOESY, and ¹⁵N-NOESY spectra were also acquired on a Bruker Avance 800-MHz spectrometer. All 3D spectra were processed by NMRPIPE (14) and analyzed with PIPP (15). 2D spectra were processed and analyzed with the program FELIX 98 (Molecular Simulations, Inc.).

Assignments and Structure Calculation—Nearly complete backbone ¹H, ¹³C, and ¹⁵N NMR assignments were achieved using standard heteronuclear methodology (16) with the assistance of AUTOASSIGN (17). Slowly exchanging amide protons were identified by dissolving the lyophilized protein in D₂O and collecting ¹⁵N-HSQC spectra as a func-

* This work was supported in part by National Institutes of Health Grants NS38604 (to W. K. S.), GM55362 (to F. D. S.), and AG14363 (to M. G. Z.). The costs of publication of this article were defrayed in part by the payment of page charges. This article must therefore be hereby marked “advertisement” in accordance with 18 U.S.C. Section 1734 solely to indicate this fact.

The atomic coordinates and structure factors (code 1QM0, 1FKC, and 1FO7) have been deposited in the Protein Data Bank, Research Laboratory for Structural Bioinformatics, Rutgers University, New Brunswick, NJ (<http://www.rcsb.org/>).

¶ To whom correspondence may be addressed. Tel.: 216-368-0139; Fax: 216-368-2546; E-mail: wks3@po.cwru.edu (for W. K. S.) or fds@po.cwru.edu (for F. D. S.).

¹ The abbreviations used are: CJD, Creutzfeldt-Jakob disease; GSS, Gerstmann-Sträussler-Scheinker disease; FFI, fatal familial insomnia; PrP, prion protein; PrP^C, cellular PrP isoform; PrP^{Sc}, scrapie (proteinase-resistant) PrP isoform; hu, human; HSQC, heteronuclear single-quantum coherence; NOE, nuclear Overhauser effect; NOESY, nuclear Overhauser effect spectroscopy; 2D, two dimensional, 3D, three-dimensional; r.m.s., atomic root mean square.

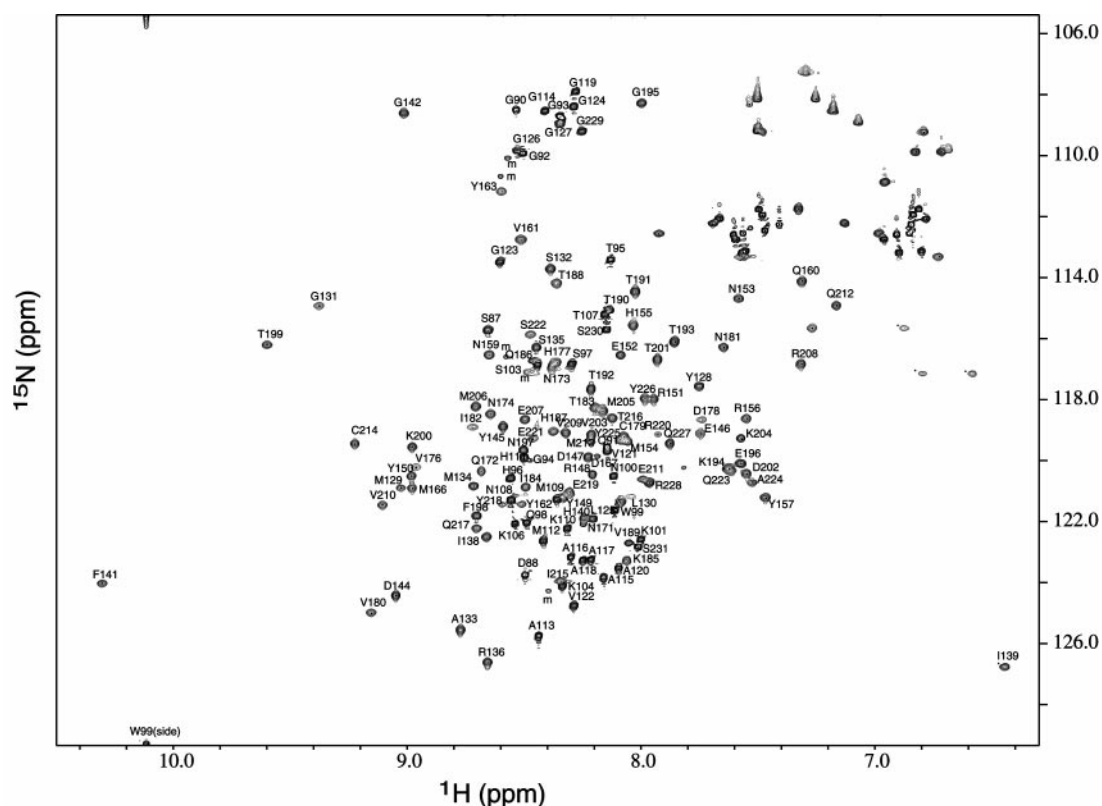


FIG. 1. ^{15}N -HSQC spectrum (800 MHz) for E200K huPrP-(90–231). With the exception of missing peaks for Arg¹⁶⁴, Tyr¹⁶⁹, Ser¹⁷⁰, and Phe¹⁷⁵, all backbone amide peaks are resolved and labeled using the single-letter amino acid code and sequence number. All expected cross-peaks for ^{15}N -containing side chains of Gln, Asn, and Arg were also assigned, although they are not labeled. Additional peaks (m) are observed because of the presence of low populations of *cis*-Xxx-Pro peptide bonds in the flexible tail of the protein.

tion of time. The NOE distance restraints were determined from 3D ^{15}N -edited NOESY (100 ms), ^{15}N -/ ^{13}C -edited NOESY (100 ms) in H_2O , ^{13}C -edited NOESY (50 and 100 ms) in D_2O , and 2D NOESY spectra (100 ms). J_{HNHA} coupling constants were measured from 3D HNHA spectra. Backbone dihedral angle restraints were added on the basis of the chemical shift indices for the H_α , C_α , and carbonyl resonances. Stereospecific assignments were obtained by direct analysis of HNHB data and short mixing time ^{13}C -NOESY (50 ms) experiments. Structure calculations were performed with the programs ARIA (18)/CNS (19) using the standard protocol, except that the upper limit for methyl groups was increased by 0.2 Å. Hydrogen-deuterium exchange rates were measured at 26 °C, and the protection factors were calculated as described previously (20).

RESULTS

The structure of the E200K variant of huPrP-(90–231) was characterized by NMR spectroscopy. In close similarity to the wild-type human (21), mouse (22), and Syrian hamster prion protein (23, 24), the N-terminal region (residues 90–124) of E200K huPrP-(90–231) is highly flexible. Present data provides no evidence of any long range interactions or local structural preferences within this part of the protein molecule. It should be noted that signal duplication observed previously for residues 120–122 in the Syrian hamster protein (23) was not found for E200K huPrP-(90–231). Multiple signals were observed for several other residues in the flexible tail, but these signals likely result from *cis* forms of three Xxx-Pro peptide bonds present in this region (Fig. 1). The solution structure was calculated for the C-terminal domain 125–231 of the mutant protein. This domain consists of three α -helices that encompass residues 144–153 (helix 1), 172–194 (helix 2), and 200–227 (helix 3) and a short β -sheet formed by two strands at residues 129–131 and 161–163 (Fig. 2). A hydrogen bond between the amide proton of Met¹³⁴ and the carbonyl oxygen of Asn¹⁵⁹ suggests the presence of an irregular, β -bulge-type elongation of the second strand.

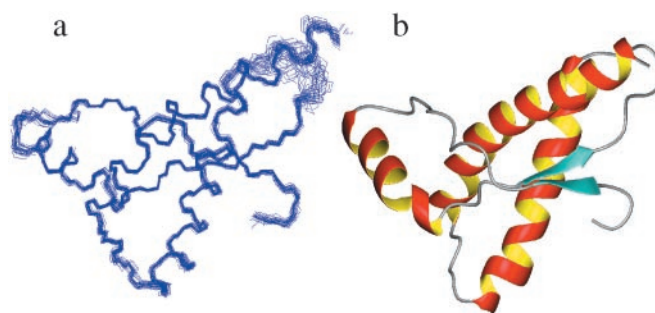


FIG. 2. The three-dimensional structure of the folded domain (residues 125–228) in E200K huPrP. *a*, the ensemble of 30 energy-minimized conformers. *b*, Richardson representation of a representative structure ($\langle \text{SA}_r \rangle$). The α -helices are colored red on the outside and yellow on the inside, whereas the β -strands are shown in cyan. The structures were displayed using the programs Insight II and MOLMOL (33).

The high quality of the present structural data is evident from statistical and PROCHECK analysis (25) (Table I). Protein regions that encompass regular secondary structure elements display very high definition (r.m.s. deviations < 0.4 Å). Loops are also well defined with r.m.s. deviations of 0.4–0.7 Å. The only undefined region in the folded domain is the loop connecting the second β -strand and helix 2 (residues 167–171). This loop is characterized by the absence of long- and medium-range NOEs. Further, the fact that some resonances in this region (such as the amide protons of Tyr¹⁶⁹ and Ser¹⁷⁰) could not be observed suggests the presence of multiple conformations, similar to the behavior of this region in the wild-type human prion protein (21).

The amide exchange (proton to deuterium) experiments established that most of the residues located within regions of well defined secondary structure are solvent-shielded. The am-

TABLE I
 Structural statistics for E200K huPrP 90–231

	<SA> ^a	<SA _r >
Experimentally derived restraints ^b		
distance restraints		
intra ($ i-j = 0$)	1070	
sequential ($ i-j = 1$)	491	
medium range ($5 > i-j > 1$)	514	
long range ($ i-j > 4$)	579	
unambiguous total	2654	
ambiguous total	516	
³ J HNHA-coupling constants	44	
H bond restraints ^c	84	
dihedral angle restraints ^d	177	
Mean r.m.s. deviations from experimental		
distance (NOE) restraints (Å)	0.0060 ± 0.0012	0.0040
dihedral restraints (degrees)	0.2908 ± 0.0508	0.2191
J-coupling restraints (Hz)	0.3438 ± 0.0709	0.2519
Mean r.m.s. deviations from idealized		
bond geometry (Å)	0.0013 ± 0.00007	0.0012
angle geometry (degrees)	0.2874 ± 0.0061	0.2744
improper geometry (degrees)	0.2192 ± 0.0094	0.1952
Energy (kcal/mol)		
total	129.57 ± 7.40	111.48
bonds	2.97 ± 0.33	2.35
angles	39.35 ± 1.67	35.85
improper	6.99 ± 0.60	5.54
Van der Waals ^e	67.89 ± 3.84	59.06
NOE	6.01 ± 2.43	2.61
dihedral	0.94 ± 0.36	0.52
Measures of structure quality ^f		
Residues in most favorable region	85.7	89.6
Residues in additional allowed region	12.9	10.4
Residues in generously allowed regions	0.8	0
Residues in disallowed regions	0.6	0
Coordinate precision ^g (Å)	125–231	125–166; 171–228
backbone	0.81 ± 0.14	0.45 ± 0.09
heavy	1.17 ± 0.12	0.83 ± 0.09

^a <SA> represents the 30 best structures of 60 calculated structures; <SA_r> indicates the structure with lowest energy. The structures were calculated with ARIA/CNS (18, 19) using energy terms for NOE distance restraints, dihedral angle restraints, bonds, angles, impropers, and hard sphere Van der Waals radii.

^b No distance restraints or dihedral angle restraints were violated by more than 0.2 Å or 3°, respectively.

^c 39 unambiguous and 3 ambiguous H bonds, two restraints per residue.

^d 67 phi, 67 psi, and 43 chi1.

^e A quartic repel potential was used in the calculations. Reported values were obtained with a final radius scaling constant of 1. Calculations were also performed with several other scaling factors between 0.78 and 1, without any noticeable effect on convergence or structural quality.

^f The overall quality of the structure was assessed using the program PROCHECK (25).

^g r.m.s. deviations for the best 30 structures selected from the total ensemble of 60 calculated structures.

ide proton exchange protection factors for these residues are very similar to those reported for the wild-type human PrP (21). However, some parts of helices show surprisingly little protection from the exchange. In particular, the C-terminal portions of helix 2 (residues 187–194) and helix 3 (residues 222–227) undergo essentially complete isotope exchange within less than 30 min, suggesting relatively large conformational flexibility in these regions. A similar finding was reported for the wild-type human PrP (21).

Overall, the 3D structure of the folded domain of E200K huPrP appears to be essentially identical to the structure previously reported for wild-type human prion protein (21) (Fig. 3). The boundaries between the secondary structure elements in these structures differ by one residue at most. The backbone r.m.s. differences are smaller than 2 Å for the entire folded domains and less than 1.5 Å for the non-loop regions. Slight differences seen among the structures (Fig. 3a) are limited to loop 167–171, the first three residues in the loop connecting strand 1 and helix 1, and the C terminus of helix 2. However, factors such as flexibility and conformational averaging (see above) limit the accuracy of structural data for these regions in both the wild-type and mutant prion protein.

Residue 200 is located at the beginning of helix 3 and is fully accessible to the solvent (Fig. 3b). It is remarkable that the local structures of the wild-type and mutant protein in the vicinity of this residue are very similar. The only observable

difference is the loss of salt-bridge interaction between the side chains of Glu²⁰⁰ and Lys²⁰⁴. In the wild-type protein, these side chains are intimately juxtaposed (within 5 Å) and therefore could be involved in a salt bridge (Fig. 3c). In the mutant protein, the nearest negatively charged side chain to Lys²⁰⁰ is that of Asp¹⁹⁶. However, these two side chains are 13 Å apart and thus too far for salt-bridge formation.

Despite the essentially identical three-dimensional structure of the wild-type and mutant prion PrP, the Glu²⁰⁰ → Lys substitution has a major effect on the distribution of charges on the protein surface. At neutral pH values, the wild-type protein surface around Glu²⁰⁰ is characterized by largely negative electrostatic potential (Fig. 4). The E200K mutation breaks the relatively uniform distribution of charges, introducing patches of positive potential. The effect is even more dramatic under mildly acidic conditions (pH around 5) that lead to the protonation of His residues. Under such conditions, the surface around residue 200 in the wild-type protein contains patches of both negative and positive electrostatic potential, whereas the mutant protein surface is predominantly positively charged (Fig. 4).

DISCUSSION

It is believed that transmissible spongiform encephalopathies are caused by a conversion of cellular prion protein, PrP^C, into a conformationally altered form, PrP^{Sc} (1–3). Of special

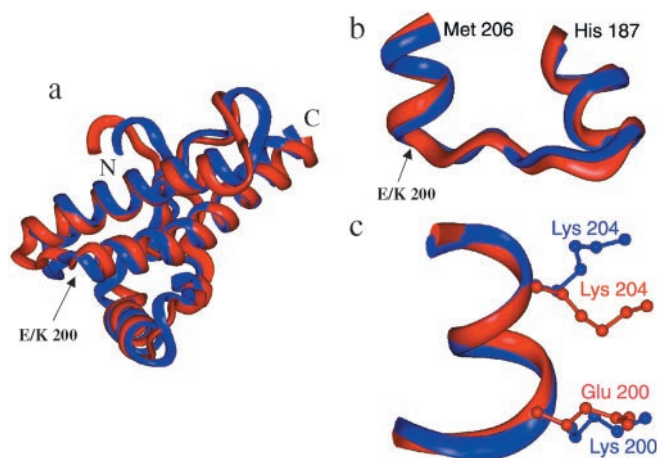


FIG. 3. Comparison of the structures for the wild-type human prion protein (21) (red) and E200K huPrP (blue). Coordinates for the wild-type protein were taken from the Protein Data Bank, accession code 1QM0. *a*, ribbon presentation for the C-terminal domain based on a best-fit superposition of residues 125–228. *b*, the best-fit superposition of residues 187–206 shows the identical backbone conformations in this region. *c*, close-up view of the mutation site in both proteins, highlighting the side chain conformation of residues 200 and 204.

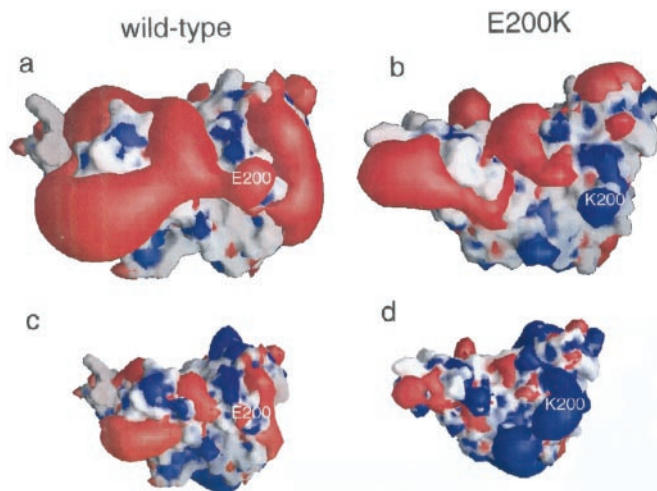


FIG. 4. The electrostatic potential for the residue 200-containing surface in the folded domain of the wild-type huPrP (left) and E200K huPrP (right). The potentials in the two upper panels (*a* and *b*) were calculated with His side chains unprotonated (neutral pH), whereas those in the bottom panels (*c* and *d*) were calculated with His side chains protonated. Blue and red colors represent positive and negative potential, respectively. The potentials were calculated at 2 kT using the program GRASP (34).

interest are familial (hereditary) forms of the disease that are associated with specific mutations in the PrP gene. Because the PrP^C → PrP^{Sc} conversion in hereditary diseases appears to occur spontaneously (*i.e.* not requiring infection with exogenous PrP^{Sc}), understanding how familial mutations affect the conformational structure and biophysical properties of prion protein should provide important clues regarding the molecular basis of the disease. It has been previously postulated that these mutations may facilitate the conversion reaction by destabilizing the native structure of PrP^C (26, 27). However, recent biophysical studies showed that many of disease-associated mutations have essentially no effect on the thermodynamic stability of the recombinant PrP, suggesting that not all hereditary prion disorders can be rationalized through a common mechanism based on thermodynamic destabilization of the cellular prion protein (28, 29). To gain further insight into the structural basis of hereditary transmissible spongiform

encephalopathies, here we have determined the solution structure of the prion protein containing a Glu²⁰⁰ → Lys mutation that is associated with the familial form of CJD. Although Glu²⁰⁰ → Lys substitution has very little effect on the thermodynamic stability of prion protein (28, 29), numerous observations argue for a causative role of this mutation in Creutzfeldt-Jakob disease. In particular, carriers of Glu²⁰⁰ → Lys mutation who live sufficiently long appear to invariably develop CJD and the resulting neuronal degeneration (30).

A striking result of the present study is the finding that the three-dimensional structure of the E200K variant is essentially identical to that previously reported for the wild-type prion protein. The only major consequence of the Glu²⁰⁰ → Lys substitution appears to be the redistribution of surface charges, resulting in a dramatically altered electrostatic potential in the mutant protein. The above surface-restricted changes are unlikely to affect the folding pattern or conformational transitions of an isolated protein molecule. Such changes could, however, have a profound effect on the ability of PrP^C to interact with other molecules present in a complex cellular environment. In particular, mutation-dependent surface effects could facilitate the conversion reaction by inducing abnormal interactions of E200K PrP^C with Protein X or other chaperones implicated in the pathogenesis of prion disorders (31, 32). The Glu²⁰⁰ → Lys replacement could also contribute to the pathogenic process by interfering with normal membrane interactions of PrP^C. The latter possibility is especially likely in view of recent data indicating that the stability and conformational transitions of prion protein are strongly affected by electrostatic interactions with cellular membranes (13). The presence of additional positively charged patches in the E200K variant could further promote these interactions, placing the protein in an environment that is especially conducive to the transition into the pathogenic PrP^{Sc} conformation. Regardless of the specific mechanism, the present data strongly suggest that mutation-dependent surface effects that may lead to abnormalities in cellular interactions of prion protein should be considered key determinants of a spontaneous PrP^C → PrP^{Sc} conversion in the E200K form of familial CJD.

Acknowledgments—We thank Drs. Chunhua Yuan and Chuck Cottrell for assistance with 800-MHz spectra acquisition and Frank Delaglio, Dan Garrett, and J. P. Linge for helpful comments.

REFERENCES

- Prusiner, S. B. (1998) *Proc. Natl. Acad. Sci. U. S. A.* **95**, 13363–13383
- Horiuchi, M., and Caughey, B. (1999) *Structure* **7**, R231–R240
- Prusiner, S. B. (1982) *Science* **216**, 136–144
- Stahl, N., Baldwin, M. A., Teplow, D. B., Hood, L., Gibson, B. W., Burlingame, A. L., and Prusiner, S. B. (1993) *Biochemistry* **32**, 1991–2002
- Meyer, R. K., McKinley, M. P., Bowman, K. A., Braunfeld, M. B., Barry, R. A., and Prusiner, S. B. (1986) *Proc. Natl. Acad. Sci. U. S. A.* **83**, 2310–2314
- Oesch, B., Westaway, D., Walchli, M., McKinley, M. P., Kent, S. B., Aebersold, R., Barry, R. A., Tempst, P., Teplow, D. B., and Hood, L. E. (1985) *Cell* **40**, 735–746
- Pan, K. M., Baldwin, M., Nguyen, J., Gasset, M., Serban, A., Groth, D., Mehlhorn, I., Huang, Z., Fletterick, R. J., Cohen, F. E., and Prusiner, S. B. (1993) *Proc. Natl. Acad. Sci. U. S. A.* **90**, 10962–10966
- Caughey, B. W., Dong, A., Bhat, K. S., Ernst, D., Hayes, S. F., and Caughey, W. S. (1991) *Biochemistry* **30**, 7672–7680
- Safar, J., Roller, P. P., Gajdusek, D. C., and Gibbs, C. J., Jr. (1993) *Protein Sci.* **2**, 2206–2216
- Riek, R., Hornemann, S., Wider, G., Billeter, M., Glockshuber, R., and Wuthrich, K. (1996) *Nature* **382**, 180–182
- Bueler, H., Aguzzi, A., Sailer, A., Greiner, R. A., Autenried, P., Aguet, M., and Weissmann, C. (1993) *Cell* **73**, 1339–1347
- Prusiner, S. B. (1994) *Proc. Natl. Acad. Sci. U. S. A.* **91**, 4611–4614
- Morillas, M., Swietnicki, W., Gambetti, P., and Surewicz, W. K. (1999) *J. Biol. Chem.* **274**, 36859–36865
- Delaglio, F., Grzesiek, S., Vuister, G. W., Zhu, G., Pfeifer, J., and Bax, A. (1995) *J. Biomol. NMR* **6**, 277–293
- Garrett, D. S., Powers, R., Gronenborn, A. M., and Clore, G. M. (1991) *J. Magn. Reson.* **95**, 214–220
- Bax, A., and Grzesiek, S. (1993) *Acc. Chem. Res.* **26**, 131–138
- Zimmerman, D. E., Kulikowski, C. A., Huang, Y., Feng, W., Tashiro, M., Shimotakahara, S., Chien, C., Powers, R., and Montelione, G. T. (1997) *J. Mol. Biol.* **269**, 592–610

18. Nilges, M., Macias, M. J., O'Donoghue, S. I., and Oschkinat, H. (1997) *J. Mol. Biol.* **269**, 408–422
19. Brunger, A. T., Adams, P. D., Clore, G. M., DeLano, W. L., Gros, P., Grosse-Kunstleve, R. W., Jiang, J. S., Kuszewski, J., Nilges, M., Pannu, N. S., Read, R. J., Rice, L. M., Simonson, T., and Warren, G. L. (1998) *Acta Crystallogr. Sect. D Biol. Crystallogr.* **54**, 905–921
20. Bai, Y., Milne, J. S., Mayne, L., and Englander, S. W. (1993) *Proteins* **17**, 75–86
21. Zahn, R., Liu, A., Luhrs, T., Riek, R., von Schroetter, C., Lopez Garcia, F., Billeter, M., Calzolari, L., Wider, G., and Wuthrich, K. (2000) *Proc. Natl. Acad. Sci. U. S. A.* **97**, 145–150
22. Riek, R., Hornemann, S., Wider, G., Glockshuber, R., and Wuthrich, K. (1997) *FEBS Lett.* **413**, 282–288
23. Liu, H., Farr-Jones, S., Ulyanov, N. B., Llinas, M., Marqusee, S., Groth, D., Cohen, F. E., Prusiner, S. B., and James, T. L. (1999) *Biochemistry* **38**, 5362–5377
24. Donne, D. G., Viles, J. H., Groth, D., Mehlhorn, I., James, T. L., Cohen, F. E., Prusiner, S. B., Wright, P. E., and Dyson, H. J. (1997) *Proc. Natl. Acad. Sci. U. S. A.* **94**, 13452–13457
25. Laskowski, R. A., Rullmann, J. A., MacArthur, M. W., Kaptein, R., and Thornton, J. M. (1996) *J. Biomol. NMR* **8**, 477–486
26. Huang, Z., Gabriel, J. M., Baldwin, M. A., Fletterick, R. J., Prusiner, S. B., and Cohen, F. E. (1994) *Proc. Natl. Acad. Sci. U. S. A.* **91**, 7139–7143
27. Cohen, F. E., Pan, K. M., Huang, Z., Baldwin, M., Fletterick, R. J., and Prusiner, S. B. (1994) *Science* **264**, 530–531
28. Swietnicki, W., Petersen, R. B., Gambetti, P., and Surewicz, W. K. (1998) *J. Biol. Chem.* **273**, 31048–31052
29. Liemann, S., and Glockshuber, R. (1999) *Biochemistry* **38**, 3258–3267
30. Chapman, J., Ben-Israel, J., Goldhammer, Y., and Korczyn, A. D. (1994) *Neurology* **44**, 1683–1686
31. Kaneko, K., Zulianello, L., Scott, M., Cooper, C. M., Wallace, A. C., James, T. L., Cohen, F. E., and Prusiner, S. B. (1997) *Proc. Natl. Acad. Sci. U. S. A.* **94**, 10069–10074
32. DeBurman, S. K., Raymond, G. J., Caughey, B., and Lindquist, S. (1997) *Proc. Natl. Acad. Sci. U. S. A.* **94**, 13938–13943
33. Koradi, R., Billeter, M., and Wuthrich, K. (1996) *J. Mol. Graph.* **14**, 51–55
34. Nicholls, A., Sharp, K. A., and Honig, B. (1991) *Proteins* **11**, 281–296